

ORIGINAL ARTICLE

In vivo morphometric analysis of inflammatory condylar changes in rat temporomandibular joint

Y Kuroki¹, K Honda^{2,5}, N Kijima¹, T Wada¹, Y Arai², N Matsumoto^{3,6}, K Iwata^{4,7}, T Shirakawa^{1,8}

Departments of ¹Pediatric Dentistry, ²Oral and Maxillofacial Radiology, ³Pathology, and ⁴Physiology, Nihon University School of Dentistry, Tokyo, Japan; Divisions of ⁵Advanced Dental Treatment, ⁶Immunology and Pathobiology, ⁷Functional Morphology, and ⁸Oral and Craniomaxillofacial Research, Dental Research Center, Nihon University School of Dentistry, Tokyo, Japan

OBJECTIVE: Injection of complete Freund's adjuvant (CFA) into the temporomandibular joint (TMJ) causes acute swelling around the joint and subsequent morphological alterations in the condyle. We aimed to evaluate changes in the three-dimensional architecture of the condyle induced with CFA.

MATERIALS AND METHODS: The CFA was injected into the unilateral TMJ of rats and morphological changes in the condyle were assessed repeatedly for 14 days by *in vivo* micro-CT.

RESULTS: Osseous abnormalities of condyle were first observed at 3–5 days after CFA injection on the tomographic images, and the condylar deformation became more obvious thereafter. Among 12 condyles examined at 14 days postinjection, osteophytosis was observed in all of the specimens and bone erosion coexisted in five condyles. None of the saline-treated condyles showed architectural changes. Significant changes were detected in the mesiolateral and rostrocaudal widths of the CFA-treated condyles at 10–14 days postinjection ($P < 0.01$). The extent of both condylar bone formation and resorption was greater in the CFA-injected TMJs than in saline-injected TMJs ($P < 0.05$).

CONCLUSION: These results indicate that CFA causes dynamic morphological changes in the condyle and that our experimental approach will provide new insights into the subacute inflammatory processes in the TMJ.

Oral Diseases (2011) 17, 499–507

Keywords: temporomandibular joint; condyle; *in vivo* micro-computed tomography; complete Freund's adjuvant; inflammation

Introduction

Injection of an adjuvant into or in the vicinity of the temporomandibular joint (TMJ) causes acute inflammation and decrease in the condylar cartilage thickness (Mazzier *et al*, 1967; Iwata *et al*, 1999; Harper *et al*, 2001; Sato *et al*, 2005). Injection of complete Freund's adjuvant (CFA) into rat TMJ induced facial swelling around the TMJ and chromodacryorrhea in a dose-dependent manner, and food intake was significantly attenuated (Harper *et al*, 2001; Kerins *et al*, 2003). Neuronal activity in the trigeminal sensory system was significantly increased in rats after the induction of TMJ inflammation with CFA, resulting in a decrement in the head withdrawal threshold to mechanical stimulation of the face (Sato *et al*, 2005). Despite evidence that CFA causes acute inflammation and subsequent arthritic symptoms, the pattern of possible morphological changes in the TMJ after CFA injection has not been investigated because of the lack of an appropriate method of detecting morphological changes in the TMJ in animal models.

Structural changes in the human TMJ have conventionally been examined by cross-sectional tomography. Since the TMJ is the most complex joint of the human body, the capacity of the tomographic imaging system determines the diagnostic outcome of TMJ examination (Westesson, 1993). Among the X-ray tomographic systems, limited cone-beam computed tomography (CT) was shown to be advantageous for the diagnosis of diseases causing morphological changes in the TMJ (Arai *et al*, 1999; Tsiklakis *et al*, 2004; Sakabe *et al*, 2006). By this technique, precise measurement and comparison of the thickness of the roof of the glenoid fossa of the TMJ have been carried out in patients suffering from TMJ diseases (Honda *et al*, 2004; Matsumoto *et al*, 2006; Kijima *et al*, 2007).

Osseous morphology of arthritic joints (Roemer *et al*, 2005), microarchitecture of trabecular bone (Nishida *et al*, 2002), and trabecular thickness of the subchondral bone of the condyle (Chen *et al*, 2009) have been visualized in small animals by micro-CT. Recently,

Correspondence: Tetsuo Shirakawa, Department of Pediatric Dentistry, Nihon University School of Dentistry, 1-8-13 Kanda-Surugadai, Chiyoda-ku, Tokyo 101-8310, Japan. Tel: +81-3-3219-8096, Fax: +81-3-3219-8353, E-mail: shirakawa@dent.nihon-u.ac.jp

Received 14 August 2010; revised 3 November 2010; accepted 18 November 2010

in vivo micro-CT (R_mCT[®]; Rigaku Co., Tokyo, Japan) was developed and its usefulness for *in vivo* imaging of small animals has been reported (Arai *et al*, 2005; Kameoka *et al*, 2009). R_mCT employs the technology used in limited cone-beam CT for human use and enables *in vivo* analysis of three-dimensional bone architecture in small animals with much higher spatial resolution than conventional micro-CT. In the present study, we injected CFA into rat TMJ and assessed subacute morphological changes in the condyle using R_mCT. TMJ scanning was performed at 1, 2, 3, 5, 7, 10, 12, and 14 days after CFA injection under pentobarbital anesthesia, and the data were analyzed by statistical methods.

Materials and methods

Experimental animals

We used 8- or 9-week-old male Sprague–Dawley rats weighing 250–350 g (SLC, Hamamatsu, Japan) in this study. They were housed in a temperature-controlled animal room (24°C), maintained on a 12:12-h light-dark cycle, and provided with pelleted food (PicoLab Rodent Diet 20[®]; PMI Nutrition International, Richmond, IN, USA) and tap water *ad libitum*. All experiments were approved by the Animal Experimentation Committee at the Nihon University School of Dentistry and the treatment of the animals conformed to the guidelines of International Association for the Study of Pain (Zimmermann, 1983).

Injection of CFA into the TMJ cavity

Rats were anesthetized with sodium pentobarbital (50 mg kg⁻¹, i.p.). First, we performed imaging of the TMJ with an injection of a contrast medium into the articular cavity of the test animals under radioscopic guidance with R_mCT (Figure 1). Running R_mCT in the fluoroscopic mode, 50 µl of the contrast medium (Optiray 320; Tyco Healthcare Japan, Tokyo, Japan) was injected into the articular cavity and an appropriate needle position was determined. CFA (heat-killed *Mycobacterium tuberculosis*, F5881; Sigma-Aldrich, Tokyo, Japan) was injected into the anesthetized rats by placing the tip of a 26-gauge needle in the articular cavity of the unilateral TMJ under radioscopic guidance with R_mCT. Animals were randomly assigned to one of the following two groups: (1) A quantity of 50 µl of CFA (1 mg ml⁻¹) suspended in oil/saline (1:1) emulsion was injected into the TMJ cavity (CFA group, *n* = 12) and (2) A quantity of 50 µl of saline was injected into the TMJ cavity (Saline group, *n* = 12). In each group, the solution was injected into either the left or the right TMJ (*n* = 6 for each side) and the other TMJ was left intact.

Measurement of lateral facial temperature over the TMJ region

In a temperature-controlled experimental room (24°C), lateral facial temperature over the TMJ region was measured by computer-assisted infrared thermography (Thermotracer TH3100ME; NEC-SANEI, Tokyo,

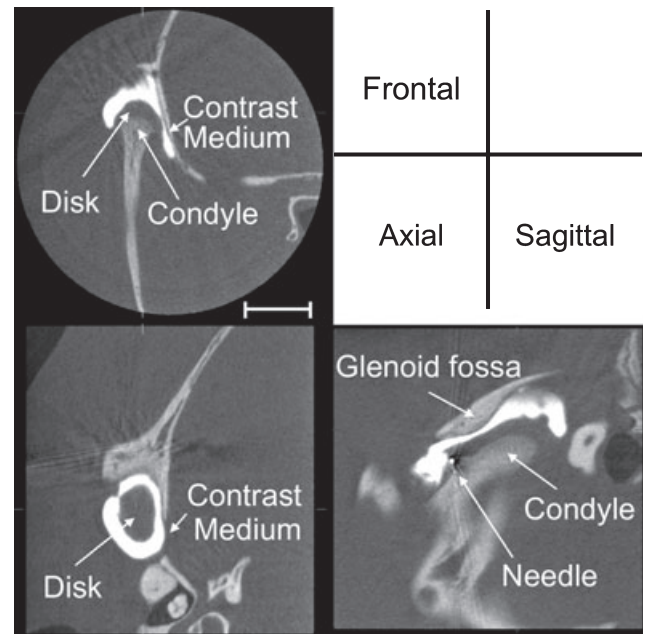


Figure 1 TMJ tomograms of a rat injected with contrast medium. In the frontal, axial, and sagittal images, the articular cavity is visualized with contrast medium as a radiopaque area. The tip of the needle used for injection is evident on the sagittal image. Scale bar = 3 mm

Japan) following tomographic TMJ imaging. The thermographic camera was fixed above the anesthetized rat and the facial temperature was measured on both CFA-injected (ipsilateral) and non-injected (contralateral) sides (Figure 2). The rat's body was supported by soft pads so that the unilateral TMJ was positioned in the center of the focus area. The increase in temperature around the ipsilateral TMJ was evaluated by subtracting the temperature value of the contralateral side from that of the ipsilateral side.

Assessment of body weight change after CFA injection

Body weight of rats was measured following the measurement of the lateral facial temperature. An automatic weighing machine (range: 0–500 g, sensitivity: 0.1 g) was used for the measurement. The change in body weight after CFA injection was assessed by subtracting the body weight value before the CFA injection from each of the postinjection values. Body weight of saline-injected rats was assessed in the same way.

Imaging of the CFA-injected TMJs using R_mCT

R_mCT is equipped with a microfocus X-ray tube fixed on one side of an I-arm providing a microfocus of 20 µm (minimum microfocus size, 7 µm). A flat panel X-ray detector (voxel size, 30 × 30 × 30 µm) was fixed on the opposite side of the I-arm 496 mm away from the X-ray tube, and the anesthetized rat was placed between the tube and the detector. To obtain appropriate CT images of rat TMJ, the voltage of the X-ray tube and the tube current were set at 90 kV and 177 µA, respectively. During X-ray irradiation for 17 s, the X-ray tube and

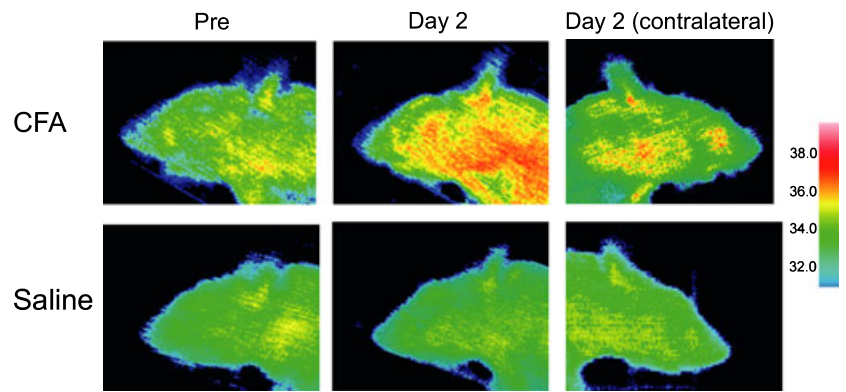


Figure 2 Typical examples of the lateral facial temperature measurement immediately before (Pre) and 2 days after (Day 2) CFA injection into the left articular cavity

the detector rotated 360° around the animal in the vertical plane, and projection data comprising 512 frames (cylindrical area; diameter, 14.4 mm and height, 14.4 mm) were collected.

Running R_mCT in the CT mode, TMJ scanning was performed 10 times in each animal; before and after placing the needle into the cavity for CFA injection and at 1, 2, 3, 5, 7, 10, 12, and 14 days after CFA injection. Animals received approximately 5 mSv radiation in a single X-ray exposure; thereby, the total radiation dose per animal in this experiment was estimated to be 50 mSv. Two-dimensional analysis of tomographic condylar images and reconstruction of three-dimensional images (size, 480 × 480 × 480 voxels) were performed using I-View-R® software (Rigaku Co.).

Stereoscopic observation of the condyles

After final TMJ examination using R_mCT, the rats were euthanized with an overdose of sodium pentobarbital. The mandible was removed from the cranium and fixed overnight with 10% formalin. Soft tissues surrounding the mandible were then removed using tweezers, and the bone was immersed overnight in a 5% sodium hypochlorite solution. After washing with distilled water, the specimen was dried and the condyles were photographed using a stereoscope. The condylar photographs were then compared with the reconstructed three-dimensional condylar images.

Histological examination of the TMJ

Fourteen days after CFA or saline injection, rats were decapitated and the heads were fixed in 10% buffered formalin. After 5 days fixation, temporal and buccinator muscles were exposed and the heads were decalcified in 10% ethylenediaminetetraacetic acid (pH: 7.5) aqueous solution for 1 week. The tissues were dehydrated in graded ethanol (70–100%), clarified in xylene and embedded in paraffin. Embedded tissues were sliced in 4 μm thickness until temporomandibular joint appeared. Tissue sections were then mounted on charged slides and stained with hematoxylin and eosin with conventional methods.

Morphometric analysis of the condyles

By using I-View-R, the TMJ was sectioned into the frontal, axial, and sagittal plane for longitudinal com-

parison of its three-dimensional architecture (Figure 1). The frontal plane was determined by searching the thickest region of the condylar head relative to the reconstructed three-dimensional condylar images. The sagittal plane was adjusted on the frontal sections such that it was positioned vertically through the center of the condyle. The axial plane was adjusted on the frontal sections such that it was positioned horizontally through the center of the condylar head. Through these processes, the best matched frontal, sagittal, and axial images were selected at each time point for the measurements.

Changes in the mesiolateral and rostrocaudal condylar widths

The width of the superior joint space (w1), mesiolateral width of the condyle (w2), mesiolateral width of the ascending mandibular ramus (w3), and rostrocaudal width of the condyle (w4) were measured on the condylar images (Figure 3). On the frontal image, w3 was determined 4 mm inferior to the surface of the condylar apex. Numerical value of the changes in the width at each measurement site was determined by calculating the absolute difference of actual values on the TMJ images obtained before and after CFA injection. The magnitude of the changes was compared between the CFA- and saline-injected rats at each point of time.

Changes in the cross-sectional bony area on condylar images

Changes in the cross-sectional bony area were examined on sagittal tomograms by an image subtraction method (Figure 4). To compare two images obtained at different points of time from the same animal, image registration was performed based on pixel domain data. By applying an edge detector to the tomographic images, the bone surface was extracted, and binary condylar images were generated. The binary images were graphically superimposed in order to maximize the overlapping (Co) area (Figure 4). When optimal position matching was achieved, the pixel numbers in the overlapping and non-overlapping areas were recorded for the analysis.

Among the non-overlapping areas, the newly formed (Ad) and resorbed (Lo) bony areas were separately

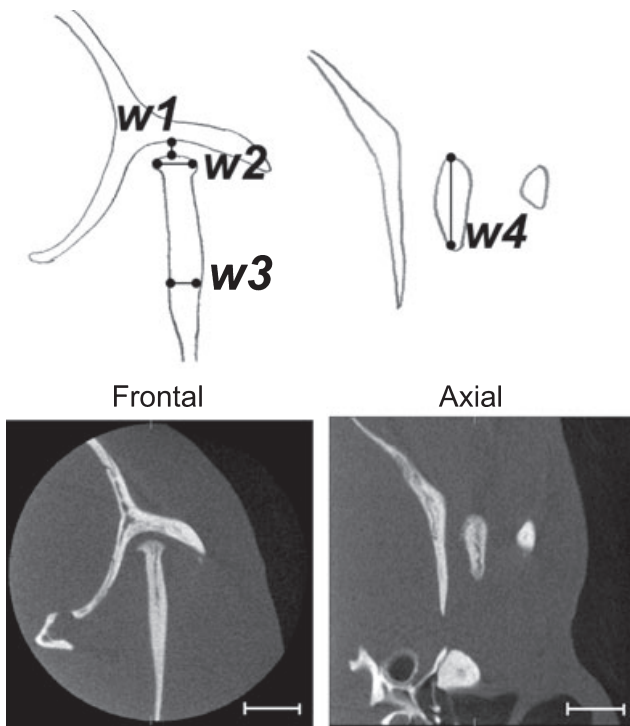


Figure 3 Measurement of the widths of the superior joint space (w1) and the condylar bone (w2, w3, w4) on the TMJ images. Scale bars = 3 mm

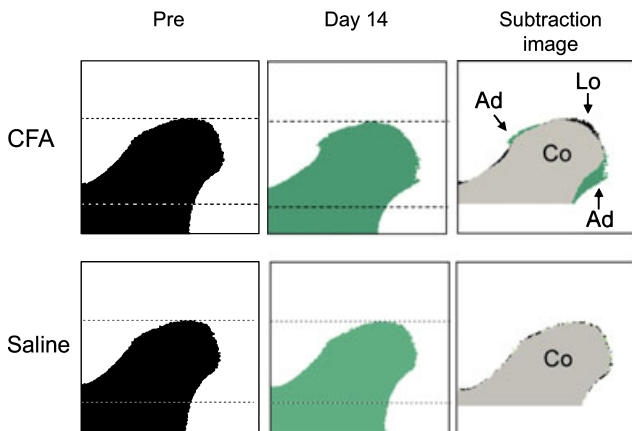


Figure 4 Detection of the additional (Ad) or lost (Lo) areas on the 2D condylar images at 14 days after CFA injection. The target areas to be analyzed are represented by dotted lines. Image subtraction method was employed for area extraction. Co: common bony area

calculated. We calculated transformation rate (Tr) as follows:

$$\text{Tr} = (\text{Ad} + \text{Lo} / \text{Ad} + \text{Lo} + \text{Co}) \times 100$$

Statistical analysis

Values are expressed as the mean \pm s.e.m. The effect of CFA injection on lateral facial temperature over the TMJ region was examined using one-way repeated-measures ANOVA followed by Dunnett's test as a *post hoc* comparison. Differences in the body weight change

during the 14-day period were compared between the CFA- and the saline-injected rats using two-way repeated-measures ANOVA.

Changes in the width of the superior joint space and in the condylar bony widths after CFA or saline injection were assessed on the tomographic images and the magnitude of changes at each point of time was compared between the two groups using the Mann-Whitney *U*-test as a statistical method. Changes in the cross-sectional bony area obtained from the condylar images were compared between the CFA- and saline-injected rats at 14 days after injection using the Mann-Whitney *U*-test. Differences were considered significant at $P < 0.05$.

Results

TMJ inflammation and body weight changes in the CFA-injected rats

All of the CFA-injected animals survived until sacrifice at 14 days postinjection. Inflammatory responses were observed in all of the CFA-injected TMJs within a day after the injection as confirmed by the thermographic observation, which revealed a rise in the temperature around the CFA-injected TMJs (Figure 2). The increase in temperature around the CFA-injected TMJs, which was evaluated by comparisons of the facial temperature of the ipsilateral and contralateral sides, was statistically significant on days 1–3 postinjection and peaked on day 2 (Figure 5a). There was no detectable change around the contralateral TMJ throughout the 14-day postinjection period.

Changes in the body weight of rats during the experimental period after CFA or saline injection are shown in Figure 5b. Both CFA- and saline-injected rats showed a decrease in their body weight during the first several days postinjection as compared to their respective preinjection levels, and the weight gradually increased thereafter. A greater decrease in body weight was noted in the CFA-injected group ($P < 0.01$).

Morphological changes in the CFA-treated condyles

Representative sagittal tomograms, reconstructed three-dimensional images, and *ex vivo* photographs of the condyles at 14 days after CFA injection are shown in Figure 6. Both tomographic condylar images and appearance of the condyles *ex vivo* indicate osseous abnormalities in the condyles injected with CFA. Osteophytosis was commonly observed in all of the CFA-treated condyles ($n = 12$) and bone erosion coexisted in five condyles. Saline injection into the articular cavity had a subtle or no detectable effect on condylar morphology (Figure 6).

Time-dependent changes in the CFA-injected TMJ

Figure 7 shows representative time-dependent changes in the CFA-treated condyles. In Figure 7a, osteophytosis was evident on day 5 postinjection and later on the tomographic images as radiopaque areas. Erosion occasionally appeared as radiolucent areas as early as day 3 postinjection, and the lesion gradually expanded

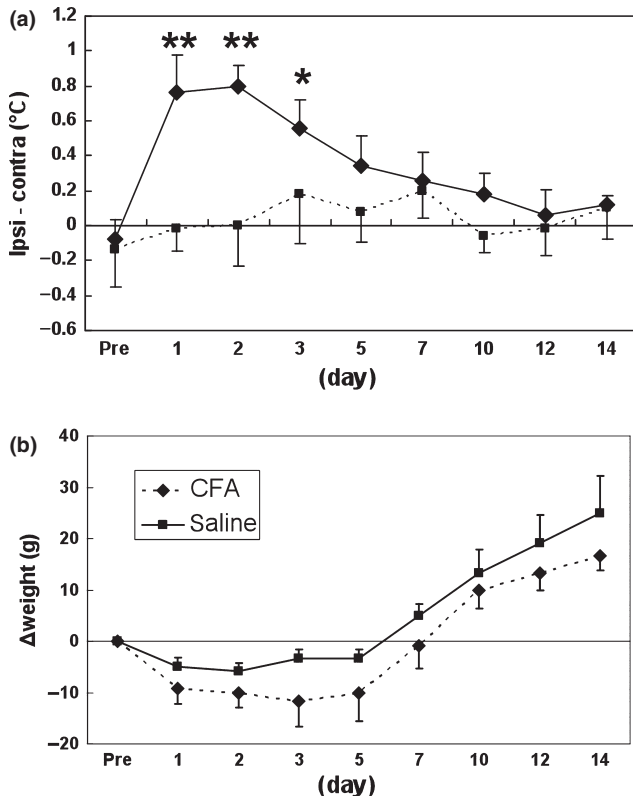


Figure 5 (a) Time-course changes in the lateral facial temperature during the 14-day period after CFA injection. Differences in the lateral facial temperature between the ipsilateral and contralateral TMJs are indicated ($n = 12$ in each group, $**P < 0.01$, $*P < 0.05$, significantly different from the preinjection level). (b) Changes in the body weight of rats during the 14-day period after CFA injection. The changes in the body weight (Δ weight) differed significantly between the CFA- and saline-injected rats ($n = 12$ in each group, $P < 0.01$)

thereafter (Figure 7b). Consistency between the newly formed radiopaque or radiolucent areas on the condylar images and the corresponding osteophytosis or erosion in the *ex vivo* specimen was confirmed visually as indicated in Figure 6.

Histopathological changes in the CFA-injected TMJ

Destructive changes in the glenoid fossa and proliferative bony changes in the condyle were seen on the

sections of the CFA-injected TMJ (Figure 8). In the CFA-injected TMJ, the articular cartilage and subchondral bone of the glenoid fossa were widely destroyed and replaced with proliferated granular tissues (Figure 8a). On the highly magnified micrographs (Figure 8b,c), marked reduction in the cartilage thickness and migration of osteoclastic multinuclear cells were seen in the superior region of the affected condyle. The bone marrow cavity of the affected condyle was enlarged and filled with fibroblast-like cells and capillaries. In contrast to the CFA-injected TMJ, pathological changes were not seen in the saline-injected TMJ (Figure 8d-f).

Enlargement of the superior joint space of CFA-injected TMJ

The width of the superior joint space of the TMJ (w_1 , Figure 3) before CFA injection is shown in Table 1. The changes in w_1 were assessed by comparing the values measured on the tomographic images before and after CFA injection. Absolute values of the difference in w_1 (Δw_1) were significantly greater in the CFA-injected rats than in the saline-injected rats throughout the 14-day postinjection period (Figure 9a). On day 14 postinjection, the difference was 0.51 ± 0.13 mm in the CFA-injected rats while it was 0.15 ± 0.03 mm in the saline-injected rats. Enlargement of the superior joint space after CFA injection was clearly visible on the sagittal images of the condyles (Figure 7).

Changes in the mesiolateral and rostrocaudal condylar widths

The mesiolateral and rostrocaudal condylar widths (w_2 , w_4) and the mesiolateral width of the ascending mandibular ramus (w_3) before CFA or saline injection are shown in Table 1. Absolute values of the difference in these bony widths after the CFA or saline injection were compared between the two groups (Figure 9b-d). The absolute values of the difference in w_2 and w_4 (Δw_2 , Δw_4) became significantly greater on day 10 postinjection and later in the CFA-injected rats compared to the saline-injected rats. There was no difference between the CFA- and saline-injected rats with regard to the absolute values of the difference in w_3 (Δw_3).

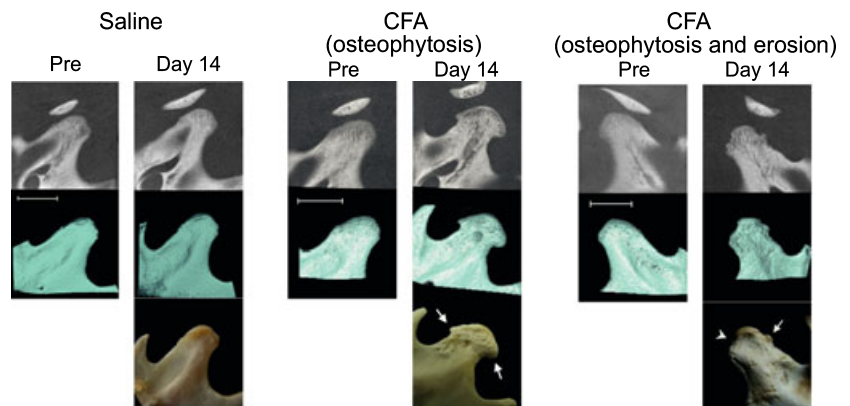


Figure 6 Sagittal tomograms, reconstructed three-dimensional images, and *ex vivo* photographs of condyles obtained before (Pre) and 14 days after (Day 14) CFA or saline injection. CFA-induced osteophytosis (arrows) and erosion (an arrowhead) in the condyle. Osteophytosis was predominantly observed. Saline injection had a subtle or no detectable effect on the condyle. Scale bars = 3 mm

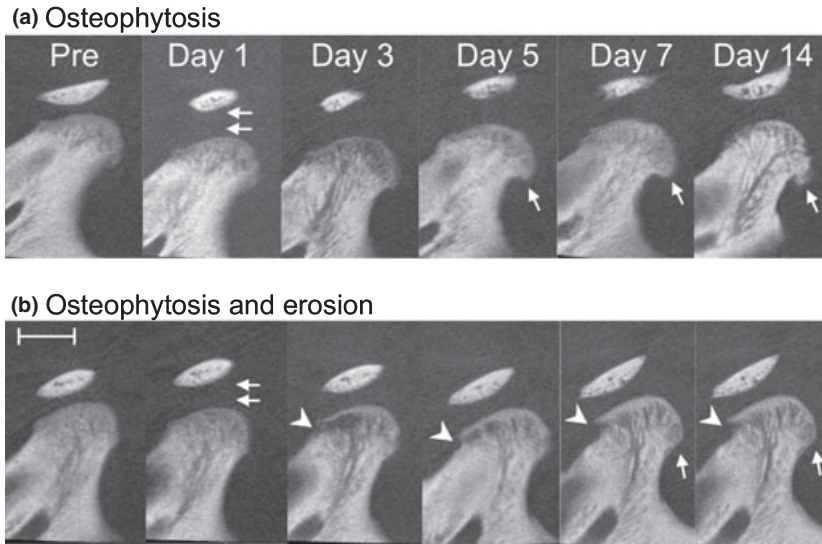


Figure 7 Time-dependent changes in the condylar morphology during the 14-day period after CFA injection. (a) Osteophytosis (single arrows) was evident at the caudal edge of the condyle on days 5–14 postinjection. (b) Erosion (arrowheads) first appeared at the rostral surface of the condyle on day 3 postinjection and gradually expanded thereafter. Double arrows indicate enlargement of the superior joint space that persisted for at least 14 days. Scale bar = 3 mm

Changes in the cross-sectional bony area on condylar images

Condylar areas of bone formation or resorption were compared between the CFA- and saline-injected rats on day 14 postinjection (Table 2). Both bone formation and resorption occurred more dynamically in the condyles of the CFA-injected rats, as compared to the saline-injected rats.

Discussion

In this study, we examined changes in the condylar architecture accompanying the TMJ inflammation. CFA

injection into the articular cavity of the TMJ caused osseous abnormalities in the condyle during the 14-day period. Morphological changes were detected on tomographic condylar images on days 3–14 postinjection, and significant changes in the mesiolateral and rostrocaudal widths of the condyle were detected on days 10–14 postinjection. Stereoscopic *ex vivo* observation of the CFA-treated condyles revealed that their morphological characteristics and surface texture were well represented on the reconstructed three-dimensional images.

No animal model of TMJ arthritis has, thus far, been shown to exhibit condylar bony changes similar to those occurring in patients suffering from TMJ arthritis

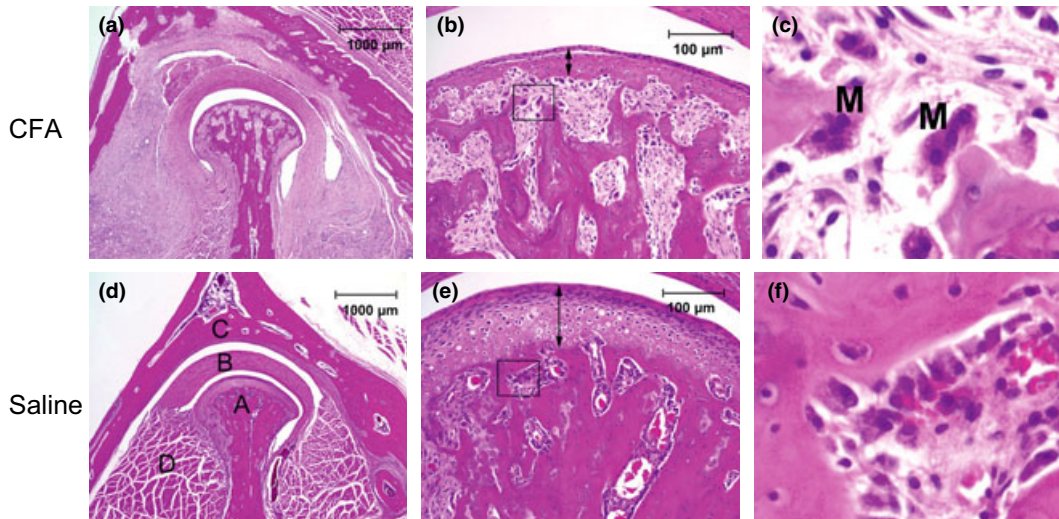


Figure 8 Histopathological changes in the CFA-injected TMJ. (a) A representative histological image of the rat TMJ at 14 days after CFA injection. (b) A higher-magnification view of the superior region of the condyle in (a). (c) A higher-magnification view of the area in (b) designated by a rectangle. (d) A representative histological image of the TMJ at 14 days after saline injection. (e) A higher-magnification view of the superior region of the condyle in (d). (f) A higher-magnification view of the area in (e) designated by a rectangle. Arrows in (b) and (e) designate the area of the condylar cartilage. The articular cartilage thickness in (b) was remarkably reduced compared to that in (e). Under microscopic observation, no inflammation related cells were observed in the condylar area. A: condyle, B: temporomandibular joint disk, C: glenoid fossa, D: lateral pterygoid muscle, M: multinuclear osteoclasts

Table 1 Initial body weight and condylar bony widths of rats

Group	n	Body weight (g)	Width (mm)			
			w1	w2	w3	w4
Saline-injected	12	285.0 ± 7.3	0.90 ± 0.03	1.67 ± 0.02	0.83 ± 0.03	2.81 ± 0.06
CFA-injected	12	291.3 ± 4.4	1.00 ± 0.07	1.66 ± 0.03	0.90 ± 0.04	2.83 ± 0.05

Data are expressed as the mean ± s.e.m. No significant differences were observed between the two groups with regard to body weight and w1–w4 before CFA injection.

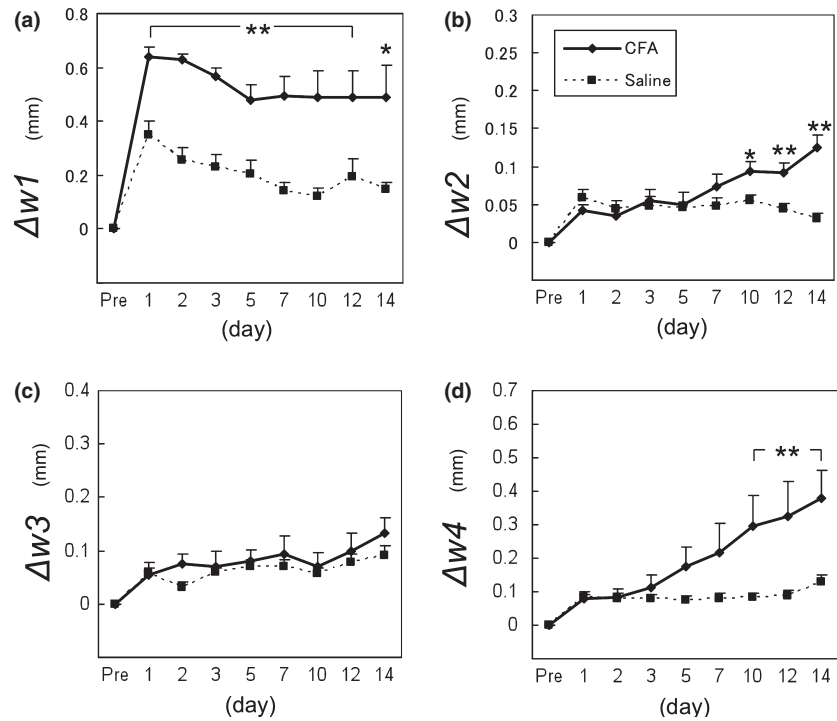


Figure 9 Effects of CFA injection on the widths of the superior joint space and condylar bone. (a) The changes in w1 ($\Delta w1$) were significantly greater in the CFA-injected rats than in the saline-injected rats throughout the 14-day period. (b) and (d) The changes in w2 and w4 ($\Delta w2$, $\Delta w4$) were significantly greater in the CFA-injected rats on day 10 postinjection and later. (c) The changes in w3 ($\Delta w3$) did not differ significantly between the two groups. $n = 12$ in each group, $**P < 0.01$, $*P < 0.05$

Table 2 Changes in the cross-sectional bony area on condylar images

Group	n	Ad (pixel)	Lo (pixel)	Ad - Lo (pixel)	Co (pixel)	Tr (%)
CFA	12	764.1 ± 117.9*	599.6 ± 105.4*	164.5 ± 157.1	11 327.2 ± 209.1	10.7 ± 1.1*
Saline	12	257.4 ± 34.0*	216.8 ± 31.3*	40.7 ± 62.0	11 085.3 ± 146.6	4.1 ± 0.1*

Data are expressed as the mean ± s.e.m. The extent of both newly formed (Ad) and resorbed (Lo) bone during the 14-day period was significantly greater in the CFA-treated condyles ($*P < 0.05$), and transformation rate (Tr) was also higher in the CFA-treated condyles ($*P < 0.05$). Co, common bony area.

(Lundeberg *et al*, 1996; Lai *et al*, 2006). In a recent study, a surgically prepared knee joint osteoarthritis model showed progressive articular cartilage degradation, subchondral bone sclerosis, and osteophyte formation (Hayami *et al*, 2006). In our CFA-induced TMJ arthritis model, time-dependent bony changes were detected in the condyle using *in vivo* micro-CT. Both bone formation and resorption occurred dynamically in the condyles of CFA-injected rats during the 14-day period. We consider that this animal model is suitable for research on the mechanism of arthritic destruction of the condyle, and *in vivo* micro-CT offers a way to assess such changes over time.

Injection of CFA into the TMJ caused various acute inflammatory changes in the TMJ region. TMJ swelling and chromodacryorrhea were induced in a dose-dependent manner, and food intake was significantly attenuated on the first day postinjection (Harper *et al*, 2001) which was in accordance with our results regarding body weight changes after CFA injection. Zhou *et al* (1999) described that TMJ inflammation peaked at 1–3 days after CFA injection. We found that injection of CFA into the TMJ caused an acute increase in the local temperature, as reported previously (Suzuki *et al*, 2007); the temperature increase was significant on days 1–3 and peaked on day 2 postinjection. Taken together,

CFA elicits acute inflammatory responses within 24 h, and the inflammation peaks by day 3 postinjection. Bony changes in the condyle become obvious thereafter.

CFA-induced TMJ inflammation continued for at least 14 days and resulted in persistent orofacial hyperalgesia in rats (Imbe *et al*, 2001). Concentrations of inflammatory mediators, such as calcitonin gene-related peptide, nerve growth factor, interleukin-1 β , and tumor necrosis factor- α , continued to be significantly elevated for 6 weeks in the TMJ tissues of the CFA-injected animals (Spears *et al*, 2005). These reports indicate that CFA has multiple and persistent effects on the tissues around the injection site, and in the present study, CFA brought about subacute inflammatory changes, such as abnormal bone formation/resorption and enlargement of the superior joint space, in the TMJ. The subacute inflammatory changes were accompanied by the reduction in the cartilage thickness and migration of osteoclastic multinuclear cells in the superior region of the affected condyle. It may be important to study the relation between the levels of inflammatory mediators and the extent of condylar changes in this animal model.

Individual bony changes in the proximal tibial metaphysis of the hind limb were measured in ovariectomized rats for 6 months by *in vivo* micro-CT (Boyd *et al*, 2006). R_mCT is suitable for detecting characteristic long-term changes in the bone architecture as well and has the advantage of a short scanning time (17 s) for a single exposure. It was demonstrated that R_mCT enabled the evaluation of the structural changes in the teeth of anesthetized rats (Osuga *et al*, 2006). The resolution of R_mCT is sufficient to detect structural changes occurring in the pulp chamber of rat molars. Performing studies using R_mCT has the advantage of reducing the number of animals required without a reduction in the detectability of subtle morphological changes. Our experimental approach will provide new insights into the subacute inflammatory processes in the TMJ.

Acknowledgements

This work was supported by KAKENHI (Grant-in-Aid for Scientific Research from the Japan Society for the Promotion of Science: 17390504, 17390555, 17591952, 18390551, 18592069); research grants from the Ministry of Education, Culture, Sports, Science, and Technology to promote multidisciplinary research projects at Nihon University; research grants for promotion of multidisciplinary research projects at Nihon University; and research grants from Sato and Uemura Funds from Nihon University School of Dentistry.

References

- Arai Y, Tammisalo E, Iwai K, Hashimoto K, Shinoda K (1999). Development of a compact computed tomographic apparatus for dental use. *Dentomaxillofac Radiol* **28**: 245–248.
- Arai Y, Yamada A, Ninomiya T, Kato T, Masuda Y (2005). Micro-computed tomography newly developed for *in vivo* small animal imaging. *Oral Radiol* **21**: 14–18.

- Boyd SK, Davison P, Müller R, Gasser JA (2006). Monitoring individual morphological changes over time in ovariectomized rats by *in vivo* micro-computed tomography. *Bone* **39**: 854–862.
- Chen J, Sorensen KP, Gupta T, Kilts T, Young M, Wadhwa S (2009). Altered functional loading causes differential effects in the subchondral bone and condylar cartilage in the temporomandibular joint from young mice. *Osteoarthritis Cartilage* **17**: 354–361.
- Harper RP, Kerins CA, McIntosh JE, Spears R, Bellinger JJ (2001). Modulation of the inflammatory response in the rat TMJ with increasing doses of complete Freud's adjuvant. *Osteoarthritis Cartilage* **9**: 619–624.
- Hayami T, Pickarski M, Zhuo Y, Wesolowski GA, Rodan GA, Duong le T (2006). Characterization of articular cartilage and subchondral bone changes in the rat anterior cruciate ligament transection and meniscectomized models of osteoarthritis. *Bone* **38**: 234–243.
- Honda K, Arai Y, Kashima M *et al* (2004). Evaluation of the usefulness of the limited cone-beam CT (3DX) in the assessment of the thickness of the roof of the glenoid fossa of the temporomandibular joint. *Dentomaxillofac Radiol* **33**: 391–395.
- Imbe H, Iwata K, Zhou QQ, Zou S, Dubner R, Ren K (2001). Orofacial deep and cutaneous tissue inflammation and trigeminal neuronal activation. Implications for persistent temporomandibular pain. *Cells Tissues Organs* **169**: 238–247.
- Iwata K, Tashiro A, Tsuboi Y *et al* (1999). Medullary dorsal horn neuronal activity in rats with persistent temporomandibular joint and perioral inflammation. *J Neurophysiol* **82**: 1244–1253.
- Kameoka S, Kuroki Y, Honda K *et al* (2009). Diagnostic accuracy of microcomputed tomography for osseous abnormalities in the rat temporomandibular joint condyle. *Dentomaxillofac Radiol* **38**: 465–469.
- Kerins CA, Carlson DS, McIntosh JE, Bellinger LL (2003). Meal pattern changes associated with temporomandibular joint inflammation/pain in rats; analgesic effects. *Pharmacol Biochem Behav* **75**: 181–189.
- Kijima N, Honda K, Kuroki Y, Sakabe J, Ejima K, Nakajima I (2007). Relationship between patient characteristics, mandibular head morphology and thickness of the roof of the glenoid fossa in symptomatic temporomandibular joints. *Dentomaxillofac Radiol* **36**: 277–281.
- Lai YC, Shaftel SS, Miller JN *et al* (2006). Intraarticular induction of interleukin-1 β expression in the adult mouse, with resultant temporomandibular joint pathologic changes, dysfunction, and pain. *Arthritis Rheum* **54**: 1184–1197.
- Lundeberg T, Alstergren P, Appelgren A *et al* (1996). A model for experimentally induced temporomandibular joint arthritis in rats: effects of carrageenan on neuropeptide-like immunoreactivity. *Neuropeptides* **30**: 37–41.
- Matsumoto K, Honda K, Sawada K, Tomita T, Araki M, Kakehashi Y (2006). The thickness of the roof of the glenoid fossa in the temporomandibular joint: relationship to the MRI findings. *Dentomaxillofac Radiol* **35**: 357–364.
- Mazzier AG, Laskin DM, Catchpole RC (1967). Adjuvant induced arthritis in the temporomandibular joint of the rat. *Arch Pathol* **83**: 543–549.
- Nishida S, Tsurukami H, Sakai A *et al* (2002). Stage-dependent changes in trabecular bone turnover and osteogenic capacity of marrow cells during development of type II collagen-induced arthritis in mice. *Bone* **30**: 872–879.

- Osuga N, Yang J, Yamakawa Y *et al* (2006). Micro-CT observation of rat dental pulp healing after pulpotomy in *in vivo* study. *Pediatr Dent J* **16**: 132–137.
- Roemer FW, Mohr A, Lynch JA, Meta MD, Guermazi A, Genant HK (2005). Micro-CT arthrography: a pilot study for the ex vivo visualization of the rat knee joint. *Am J Roentgenol* **184**: 1215–1219.
- Sakabe R, Sakabe J, Kuroki Y, Nakajima I, Kijima N, Honda K (2006). Evaluation of temporomandibular disorders in children using limited cone-beam computed tomography: a case report. *J Clin Pediatr Dent* **31**: 14–16.
- Sato T, Kitagawa J, Ren K *et al* (2005). Activation of trigeminal intranuclear pathway in rats with temporomandibular joint inflammation. *J Oral Sci* **47**: 65–69.
- Spears R, Dees LA, Sapozhnikov M, Bellinger LL, Hutchins B (2005). Temporal changes in inflammatory mediator concentrations in an adjuvant model of temporomandibular joint inflammation. *J Orofac Pain* **19**: 34–40.
- Suzuki I, Harada T, Asano M *et al* (2007). Phosphorylation of ERK in trigeminal spinal nucleus neurons following passive jaw movement in rats with chronic craniomandibular joint inflammation. *J Orofac Pain* **21**: 225–231.
- Tsiklakis K, Syriopoulos K, Stamatakis HC (2004). Radiographic examination of the temporomandibular joint using cone beam computed tomography. *Dentomaxillofac Radiol* **33**: 196–201.
- Westesson PL (1993). Reliability and validity of imaging diagnosis of temporomandibular joint disorder. *Adv Dent Res* **7**: 137–151.
- Zhou Q, Imbe H, Dubner R, Ren K (1999). Persistent Fos protein expression after orofacial deep or cutaneous tissue inflammation in rats: implications for persistent orofacial pain. *J Comp Neurol* **412**: 276–291.
- Zimmermann M (1983). Ethical guidelines for investigations of experimental pain in conscious animals. *Pain* **16**: 109–110.

Copyright of Oral Diseases is the property of Wiley-Blackwell and its content may not be copied or emailed to multiple sites or posted to a listserv without the copyright holder's express written permission. However, users may print, download, or email articles for individual use.